

Squeezing-enhanced phase-shift-keyed binary communication in noisy channels

Giovanni Chesi,¹ Stefano Olivares,^{2,3,*} and Matteo G. A. Paris^{2,3}

¹*Dipartimento di Fisica e Matematica, Università degli Studi dell'Insubria, I-22100 Como, Italy*

²*Quantum Technology Lab, Dipartimento di Fisica, Università degli Studi di Milano, I-20133 Milano, Italy*

³*INFN, Sezione di Milano, I-20133 Milano, Italy*

(Dated: December 14, 2024)

We address binary phase-shift-keyed (PSK) communication channels based on Gaussian states and prove that squeezing improves state discrimination at fixed energy of the channel, also in the presence of phase diffusion. We then assess performances of homodyne detection against the ultimate quantum limits to discrimination, and show that homodyning achieves optimality in large noise regime. Finally, we consider noise in the preparation of the *seed* signal (before phase encoding) and show that also in this case squeezing may improve state discrimination in realistic conditions.

I. INTRODUCTION

Quantum hypothesis testing addresses the discrimination of non-orthogonal preparations of a quantum system. As such, it has attracted attention from a fundamental point of view [1–9], and represents a central tool for the design and development of quantum communication channels. In particular, much attention has been paid to quantum binary discrimination, which already shows a rich quantum phenomenology amenable to analytic investigations, and fosters promising perspectives in a number of challenging applications, such as quantum communication [10, 11] and quantum cryptography [12]. In particular, quantum-optical implementations of state discrimination have been investigated [13–15], with focus on information carried by coherent states ([16, 17]), though also the use of squeezing have been explored to some extent ([18, 19]).

In quantum binary communication, one has to discriminate between two quantum signals. Assuming a pure preparation, i.e. ignoring the presence of noise, we may denote the two states by $|\psi_1\rangle$ and $|\psi_2\rangle$. The minimum error probability is not vanishing for non-orthogonal states and is given by the so-called Helstrom bound [2] (throughout the paper we assume equal prior probability for the two signals):

$$P^{(\min)}(|\psi_1\rangle, |\psi_2\rangle) = \frac{1}{2}(1 - \sqrt{1 - |\langle\psi_1|\psi_2\rangle|^2}). \quad (1)$$

In quantum communication channels the two states are often obtained from a *seed* state $|\psi_0\rangle$ through a suitable unitary transformation. In coherent-state communication, the quantum signal $|\psi_k\rangle$, $k = 1, 2$, is obtained by applying a displacement operation to the vacuum state $|0\rangle$, namely, $|\psi_k\rangle = D[(-1)^k \alpha] |0\rangle$, where $D(\alpha) = \exp(\alpha a^\dagger - \alpha^* a)$, $[a, a^\dagger] = \mathbb{I}$ and we can assume $\alpha \in \mathbb{R}$, $\alpha > 0$. Since the difference between the two states is an overall π phase, we refer to this encoding as to phase-shift keying (PSK). This channel has been thoroughly investigated because of the peculiar properties of coherent states: they can be easily generated and manipulated and their phase properties are not affected by losses (only their amplitude is reduced). Therefore, they can travel for long distances preserving their coherence properties [11, 20].

The search for optimal receivers, i.e. detection schemes and strategies able to discriminate between the two coherent states reaching the corresponding Helstrom bound, has eventually led to the so-called *Kennedy receiver* [21] and *Dolinar receiver* [22]. These are both based on the interference of the signals with a known reference, and on on/off photo-detectors, able to check the presence or absence of light. Dolinar receiver also exploits a feedback mechanism in order to achieve the Helstrom bound (it requires, however, many copies of the same input state in order to implement the feedback). These kinds of detectors require a precise phase reference control and in the presence of phase fluctuations their performances are drastically reduced [23]. On the other hand, it has been shown that in the presence of phase noise a receiver based on homodyne detection [31] allows to approach optimality [24].

Recently, coherent-state encoding and homodyne detection have been used to establish ground-satellite links [11], whereas squeezed states have been suggested to improve quantum key distribution [25]. Motivated by these results, here we consider a binary communication channel in which the seed $|\psi_0\rangle$ is a squeezed vacuum $|r\rangle = S(r)|0\rangle$ where $S(r) = \exp\{\frac{1}{2}[r(a^\dagger)^2 - r^* a^2]\}$ is the squeezing operator. Without lack of generality we assume $r \in \mathbb{R}$. In this case the input states are:

$$|\psi_1\rangle = |-\alpha, r\rangle, \quad \text{and} \quad |\psi_2\rangle = |\alpha, r\rangle. \quad (2)$$

where we introduced the displaced squeezed state (DSS) $|\beta, r\rangle = D(\beta)S(r)|0\rangle$. In the following, we will first address the Helstrom bound for two DSSs and compare the results with those obtained with coherent states and/or using homodyne detection. We then investigate the effect of phase diffusion on the discrimination and compare our results with the ultimate quantum limits, i.e. the corresponding Helstrom bound. Finally, we analyze the effect of losses, resulting in a reduced purity of the seed state.

II. DISCRIMINATION BETWEEN DISPLACED-SQUEEZED STATES

Let us start by investigating the ultimate performances of DSSs with respect to the coherent-state ones in the absence of noise and with optimal detection. This corresponds to evaluate

*Electronic address: stefano.olivares@fisica.unimi.it

the Helstrom bound for the input states given in Eqs. (2). For the sake of simplicity, we can assume $\alpha, r \in \mathbb{R}$, with $\alpha, r > 0$. The corresponding Helstrom bound can be easily calculated from Eq. (1) and reads:

$$\begin{aligned} P^{(\min)}(r, \alpha) &= \frac{1}{2} \left(1 - \sqrt{1 - |\langle \alpha, r | -\alpha, r \rangle|^2} \right) \\ &= \frac{1}{2} \left[1 - \sqrt{1 - \exp(-4\alpha^2 e^{-2r})} \right]. \end{aligned} \quad (3)$$

It is clear that for fixed coherent amplitude, squeezing always allows to improve the discrimination. However, the squeezing operation is adding energy to the coherent states, resulting in a comparison between two encodings with different total energy. A better comparison may be obtained by fixing the total energy used in the communication channel which is usually set by physical constraints. For the coherent-state channel based on $|\pm\alpha\rangle$ we have the following average number of photons $N_{\text{CS}} = |\pm\alpha|^2$, whereas, if we employ DSSs $|\pm\alpha, r\rangle$, the energy is given by $N_{\text{DSS}} = |\alpha|^2 + N_{\text{sq}}$, where $N_{\text{sq}} = \sinh^2(r)$ is the average number of photons added by the squeezing process. If we impose the constraint on the energy, we can clearly see that the more the state is squeezed the less is displaced and vice versa; hence, the discrimination problem becomes not trivial.

Our aim is to find the regimes in which squeezing can be a useful resource for the discrimination. Therefore, in the following we are going to study the error probability as a function of the introduced amount of squeezing (and at fixed total energy). Given the channel energy N and the fraction of squeezing:

$$\beta \equiv \frac{N_{\text{sq}}}{N} = \frac{\sinh^2(r)}{N}, \quad (4)$$

we can rewrite Eq. (3) expressed in terms of β and N , namely:

$$\begin{aligned} P^{(\min)}(\beta, N) &= \frac{1}{2} \left\{ 1 - \left[1 - \exp \left[-4N(1 - \beta) \right] \right. \right. \\ &\quad \left. \left. \times \left(1 + 2N\beta + 2\sqrt{N\beta + N^2\beta^2} \right) \right] \right\}^{\frac{1}{2}}. \end{aligned} \quad (5)$$

We plot the behavior of $P^{(\min)}(\beta, N)$ in the left panel of Fig. 1. We can find an interval of β values such that the error probability of a pair of DSSs is smaller than the corresponding coherent case. Then two critical values for β are naturally identified: a threshold value $\beta_{\text{th}}(N)$ and an optimum value β_{opt} . For $0 < \beta < \beta_{\text{th}}$, DSSs achieve better performances with respect to coherent states and, in particular, it is possible to minimize the error probability by choosing a suitable squeezing fraction (β_{opt}). These quantities can be obtained analytically and reads:

$$\beta_{\text{th}}(N) = \frac{4N}{4N+1}, \quad \text{and} \quad \beta_{\text{opt}}(N) = \frac{N}{2N+1}, \quad (6)$$

respectively. It is straightforward to see that in the limit $N \gg 1$ one finds $\beta_{\text{th}} \rightarrow 1$ and $\beta_{\text{opt}} \rightarrow 1/2$. In this limit, the best strategy is to use the half of the channel energy for

squeezing. Moreover, we have that, for coherent states ($\beta = 0$), $P_{\text{CS}}^{(\min)} = P^{(\min)}(0, N) = \frac{1}{2} \left[1 - \sqrt{1 - \exp(-4N)} \right]$, whereas for DSSs with $\beta = \beta_{\text{opt}}$ we find $P_{\text{DSS}}^{(\min)} = P^{(\min)}(\beta_{\text{opt}}, N) = \frac{1}{2} \left[1 - \sqrt{1 - \exp[-4N(N+1)]} \right]$. Hence, in the limit $N \gg 1$ the corresponding minimum error probabilities are:

$$\begin{aligned} P_{\text{CS}}^{(\min)} &\rightarrow \frac{1}{4} \exp(-4N), \\ P_{\text{DSS}}^{(\min)} &\rightarrow \frac{1}{4} \exp[-4N(N+1)] \sim \frac{1}{4} \exp(-4N^2), \end{aligned}$$

and the clear advantage can be also highlighted by considering the following ratio:

$$\frac{P_{\text{CS}}^{(\min)}(0, N) - P_{\text{DSS}}^{(\min)}(\beta_{\text{opt}}, N)}{P_{\text{CS}}^{(\min)}(0, N)} \rightarrow 1 - \exp(-4N^2). \quad (7)$$

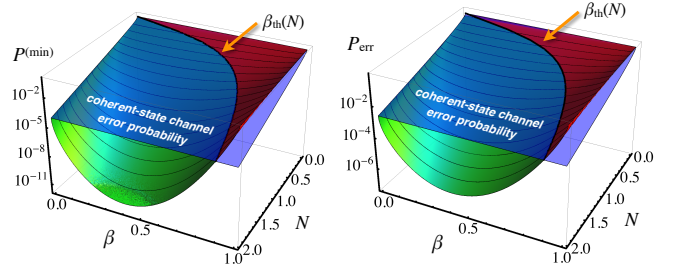


Figure 1: (Left) The Helstrom bound (5) as functions of the squeezing fraction β and the channel energy N . We also plot the plane corresponding to the Helstrom bound for coherent states. The solid line corresponds to the threshold $\beta_{\text{th}}(N)$: given the total energy N , if $\beta < \beta_{\text{th}}(N)$ the use of DSSs outperforms coherent states. (Right) The homodyne error probability P_{err} of Eq. (9) as a function of β for different values of the channel energy N . The behavior is qualitatively similar to the Helstrom bound reported in the left panel (see however the different scaling). We also plot the plane corresponding to the minimum error probability achievable using only coherent states and homodyne detection.

Let us now turn attention on feasible measurements that we can perform on our optical states in order to discriminate between them. It is well-known that in the absence of noise and in the case of just two phase-shifted coherent states there exist methods based on photon-number resolving detectors which allow one to approach the Helstrom bound [21, 22, 27, 28]. Other proposals are based on an active detection stage, namely, a squeezing operation is applied to the signal before the detection [19].

However, one has to take into account noise to describe a realistic channel. Since we chose to employ a PSK channel, information is encoded on phase, so that the most detrimental kind of noise affecting our channel is phase noise. It has been shown [24] that homodyne detection is robust against phase noise; in particular, in the limit of large noise it beats the performances of a Kennedy receiver for every value of N and achieves the Helstrom bound. These results lead us to

consider homodyne detection in order to discriminate DSSs. On the one hand, this is a standard and well-established technique when dealing with continuous-variable optical system, which is also promising in view of coherent-state communication with satellite [11]. On the other hand, homodyne detection strategy has been proved to approach the Helstrom bound when phase noise affect the signal [24, 29], which is the scenario we will discuss in the next sections.

Homodyne detection allows to measure the quadrature operator $x_\theta \equiv ae^{-i\theta} + a^\dagger e^{i\theta}$ of the input field [26], where $[a, a^\dagger] = \mathbb{I}$ and θ is the phase of the quadrature. Since we assumed real displacement amplitude and squeezing, we can focus on the measurement of x_0 . As usual the two inputs $|\pm\alpha, r\rangle$, with $\alpha, r > 0$, are sent to the receiver, which measures x and obtain the outcome $x \in \mathbb{R}$ from the homodyne detection. In order to discriminate between the two states, shot by shot, the receiver uses the following strategy:

$$\begin{cases} x \geq 0 \Rightarrow |0\rangle \equiv |\alpha, r\rangle, \\ x < 0 \Rightarrow |1\rangle \equiv |-\alpha, r\rangle. \end{cases} \quad (8)$$

The error probability associated with this strategy writes:

$$P_{\text{err}} = \frac{1}{2} [p(x \geq 0|1) + p(x < 0|0)] = p(x \geq 0|1). \quad (9)$$

where we used $p(x < 0|0) = p(x \geq 0|1)$. The conditional probabilities appearing in Eq. (9) are defined as:

$$p(x \geq 0|1) = \int_0^{+\infty} dx p^{(\text{HD})}(x; \pm\alpha, r), \quad (10)$$

where $p^{(\text{HD})}(x; \pm\alpha, r)$ is the *homodyne probability*, which reads:

$$\begin{aligned} p^{(\text{HD})}(x; \pm\alpha, r) &\equiv |0\langle x|\pm\alpha, r\rangle|^2 \\ &= \sqrt{\frac{2}{\pi}} e^{-r} \exp\left\{-\frac{[(x \pm 2\alpha)e^{-r}]^2}{2}\right\}, \end{aligned} \quad (11)$$

with $x_\theta|x\rangle_\theta = x|x\rangle_\theta$, or, in terms of the squeezing fraction β and the total number of photons N , as

$$p^{(\text{HD})}(x; \beta, N) = \sqrt{\frac{2}{\pi}} \frac{\exp\left[\frac{1}{2}\left(\frac{x-2\sqrt{N(1-\beta)}}{\sqrt{\beta N} + \sqrt{\beta N+1}}\right)^2\right]}{\sqrt{\beta N} + \sqrt{\beta N+1}}. \quad (12)$$

In the right panel of Fig. 1 we show P_{err} as a function of the squeezing fraction β and N . The plot well illustrates two features of the detection strategy. On the one hand, PSK based on DSSs outperforms the corresponding coherent protocol as far as the squeezing fraction is below a threshold value, which is the same minimising the Helstrom bound i.e. that given in Eqs. (6). Notice that being the encoding on pure states, the same working regime is also maximising the mutual information between the sender and the receiver [9]. On the other hand, upon comparing the homodyne error probability with the ultimate bound of the left panel, we see that homodyne detection does not implement the optimum receiver, since the error probability is far from approaching the Helstrom bound.

At the same time, it is known that homodyne performances with coherent encoding are useful in the presence of phase noise and, in particular, phase diffusion [24, 30]. Therefore, in the following, we are going to investigate whether the use of squeezing can further improve the discrimination between the two signals when phase noise affects their propagation.

III. DISCRIMINATION IN THE PRESENCE OF PHASE NOISE

The effect of phase diffusion on a single-mode state can be described by the the following Master equation [30, 33]:

$$\dot{\rho}(t) = \Gamma \mathcal{L}[a^\dagger a] \rho(t) \quad (13)$$

where $\rho(t)$ is the density operator of the system, $\mathcal{L}[O]\rho = 2O\rho O^\dagger - O^\dagger O\rho - \rho O^\dagger O$, and Γ is the diffusion parameter. Simple calculations provide the following solution

$$\rho(t) = \sum_{n,m} \rho_{n,m}(t) |n\rangle\langle m| = \sum_{n,m} e^{-(n-m)^2 \Delta} \rho_{n,m}(0) |n\rangle\langle m| \quad (14)$$

where $\rho_{n,m}(t) = \langle n|\rho(t)|m\rangle$ and $\Delta \equiv \Gamma t$.

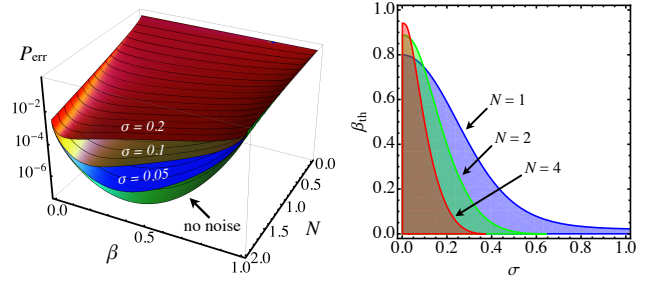


Figure 2: (Left) Error probability P_{err} of the homodyne receiver in the presence of phase diffusion as a function of β and N for different values of the noise parameter σ . (Right) Threshold value $\beta_{\text{th}}(\sigma)$ as a function of the noise parameter σ for different values of N . The shaded regions refer to the couples of parameters (σ, β) such that DDSs outperform coherent states.

Equation (14) can be rewritten in the following form:

$$\rho(t) = \int_{-\infty}^{+\infty} d\phi \frac{\exp[-\frac{\phi^2}{2\sigma^2}]}{\sqrt{2\pi\sigma^2}} U_\phi \rho(0) U_\phi^\dagger, \quad (15)$$

where we introduced the phase shift operator $U_\phi = e^{-i\phi a^\dagger a}$, $\sigma^2 = 2\Gamma t = 2\Delta$ and $\rho(0) = |\pm\alpha, r\rangle\langle\pm\alpha, r|$. From now on we will refer to σ as to the noise parameter.

Since $U_\phi|\pm\alpha, r\rangle = |\pm\alpha e^{-i\phi}, r e^{-i\phi}\rangle$, one can easily calculate the error probability after the phase diffusion process starting from the homodyne probabilities:

$$\begin{aligned} p_\sigma^{(\text{HD})}(x; \pm\alpha, r) &= \int_{-\infty}^{+\infty} d\phi \frac{\exp[-\frac{\phi^2}{2\sigma^2}]}{\sqrt{2\pi\sigma^2}} \\ &\quad \times |0\langle x|\pm\alpha e^{-i\phi}, r e^{-i\phi}\rangle|^2. \end{aligned} \quad (16)$$

In Fig. 2 (left panel) we plot the resulting error probability $P_{\text{err}}(\sigma)$ as a function of β and N for different values of the noise parameter σ : as one may expect, the error probability increases but, nevertheless, the DSSs perform better than the coherent states when β is below a new threshold $\beta_{\text{th}}(N, \sigma)$ that now depends on both N and the noise parameter σ , as shown in the right panel of Fig. 2. It is interesting to note that for large amount of phase noise $\beta_{\text{th}}(N, \sigma)$ exhibits an asymptotic behavior (see the right panel of Fig. 2): this is illustrated in the left panel Fig. 3, where we plot the asymptotic value β_{lim} as a function of N .

The presence of a non vanishing squeezing fraction can be explained considering how large phase diffusion affects the homodyne probability distribution associated with the DSS and the coherent state. An example is given in the right panel of Fig. 3: the presence of squeezing on the one hand reduces the coherent amplitude of the state and, on the other hand, enhances the asymmetry of the homodyne probability distribution. Overall, this leads to a reduction of the corresponding discrimination error probabilities, that are related to the shaded areas shown in the right panel of Fig. 3.

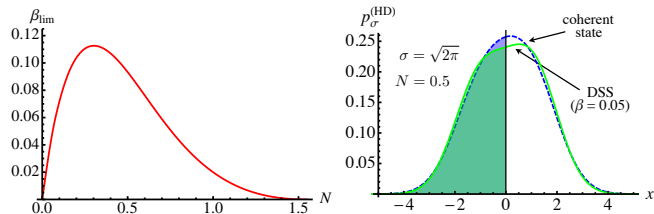


Figure 3: (Left) Asymptotic values of the squeezing fraction β_{lim} in the presence of large phase diffusion as a function of N . (Right) Homodyne probability distributions in presence of a large amount of noise ($\sigma \sim \sqrt{2\pi}$) for a coherent state (blue dashed line) and a DSS with $\beta = 0.05$ (green solid line). The total energy of the states is set to $N = 0.5$. We note the asymmetry of the two distributions, due to the phase noise, which is more enhanced in the case of the DSS: this results in a lower discrimination error probability for the DDS (green shaded area below the solid curve) w.r.t. the coherent state one (blue shaded area below the dashed curve).

A. Comparison with the ultimate bounds

Here we compare the results obtained in the previous section with the minimum error probability given by the Helstrom bound in the presence of phase noise. Given two mixed states ρ_1 and ρ_2 , the Helstrom bounds reads [2]:

$$P^{(\min)}(\rho_1, \rho_2) = \frac{1}{2} [1 - D(\rho_1, \rho_2)], \quad (17)$$

where $D(\rho_1, \rho_2) \equiv \frac{1}{2} \|\rho_1 - \rho_2\|_1$, with $\|A\|_1 = \frac{1}{2} \text{Tr} [\sqrt{A^\dagger A}]$, is the trace distance between the states ρ_1 and ρ_2 .

In Fig. 4 we compare the Helstrom bound for the DSS with the error probability obtained by using the homodyne strategy (plots on the left side of Fig. 4). As in the case of the coherent states analysed in Ref. [24], also when the binary information

is encoded in DSSs the homodyne detection approaches the optimal measurement in the presence of phase diffusion. It is however worth noting that DSSs allow to obtain a lower error probability and also to beat the Helstrom bound of the coherent-state case for small values of the noise parameter σ (see the right side of Fig. 4).

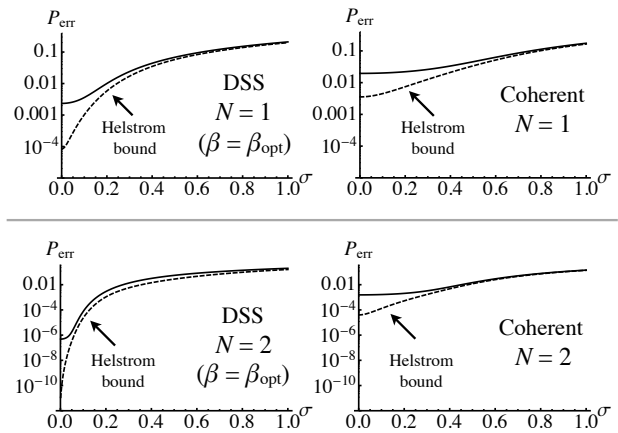


Figure 4: Comparison between the error probability P_{err} (solid lines) and the Helstrom bound (dashed lines) as functions of the noise parameter σ for the DSS and the coherent state and for two different values of the energy: (top) $N = 1$ and (bottom) $N = 2$. It is worth noting that, in the presence of small values on σ , DSSs can beat the Helstrom bound of the corresponding coherent-state channel. For the DSS we used the optimal squeezing fraction $\beta_{\text{opt}}(N)$ given in Eq. (6).

B. Effect of purity on the discrimination

The analysis we pursued in the previous sections focused on a *pure* seed state, namely the squeezed vacuum $|\psi_0\rangle = S(r)|0\rangle$. In order to take into account possible imperfections in the generation of squeezed states and losses in their propagation, we extend our analysis to include the effect of a non-unit purity $\mu = \text{Tr}[\rho_0^2]$ of the seed state which is now described by the density operator ρ_0 . Without loss of generality, we can assume that in this case the seed is given by the *squeezed thermal state* [34]:

$$\rho_0 = S(r)v(\mu)S^\dagger(r) \quad (18)$$

where $v(\mu)$ is a thermal state with average number of photons $N_{\text{th}} = (1 - \mu)/(2\mu)$. In fact, the effect of losses on a squeezed vacuum states can be summarized as an overall thermal contribution to the state (see, e.g., the experimental works in Refs. [35, 36] on the generation of single- and two-mode squeezing). In this case we can still follow the discrimination strategy mentioned above, but now the total energy of the displaced input state $D(\pm\alpha)\rho_0 D^\dagger(\pm\alpha)$ reads:

$$N = |\alpha|^2 + N\beta + \frac{1 - \mu}{2\mu} (1 + 2N\beta), \quad (19)$$

where the squeezing fraction β is the same as in Eq. (4). Note that $(1 + 2N)^{-1} \leq \mu \leq 1$. In the left panel of Fig. 5 we plot

the corresponding error probability as a function of β and the purity μ for $N = 2$ (analogous results can be found for other energies) for different values of the noise parameter σ introduced in the previous section. As expected, the presence of a mixed seed state ($\mu < 1$) increases the error probability. Nevertheless, we can find again a threshold on the squeezing parameter below which this nonclassical resource enhances the discrimination with respect to the coherent state (for the same fixed energy). The threshold now depends also on the purity of the state as shown in the right panel of Fig. 5.

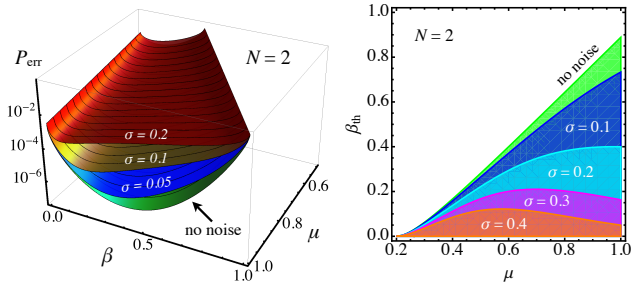


Figure 5: (Left) Error probability as a function of β and the purity μ of the seed state for different values of the noise parameter σ . We set $N = 2$. (Right) Threshold value $\beta_{\text{th}}(\mu)$ as a function of the purity μ of the states for different values of the noise parameter σ (note that $(1 + 2N)^{-1} \leq \mu \leq 1$). The shaded regions refer to the pairs of parameters (μ, β) for which DDSs outperform coherent states. Also here we set $N = 2$.

IV. CONCLUSIONS

We have investigated the role of squeezing in PSK quantum communication and shown that it represents a resource in

the presence of phase diffusion. In particular, we focused on binary encoding onto displaced squeezed states (DSSs) with coherent amplitudes having opposite phases. We have considered both the ultimate limit to the error probability given by the Helstrom bound and a realistic scenario based on homodyne detection. In absence of noise there exists a threshold value $\beta_{\text{th}}(N)$ on the squeezing fraction β : below this threshold the Helstrom bound for DSSs is lower than that obtained using coherent channels with the same energy.

When phase diffusion is taken into account, the error probability unavoidably increases. However, we can still find a threshold value $\beta_{\text{th}}(N, \sigma)$, now depending also on the phase-noise parameter σ , below which squeezing provides improvement. In the presence of large phase diffusion, the threshold approaches a non-vanishing asymptotic value, which rapidly vanishes for $N > 1$. By comparison with the Helstrom bound evaluated in the presence of phase noise, we have shown that a channel with DSSs encoding and homodyne detection approaches the optimality. On the one hand, this confirms the findings obtained with coherent encoding [24]. On the other hand, we have found that the error probability obtained exploiting the squeezing may fall below the ultimate limit given by the Helstrom bound for coherent states.

Our results put squeezing forward as a resource for quantum communication channels in realistic conditions, namely, when phase-noise and losses occur during the generation and the propagation of information carriers. They also pave the way for further developments in M -ary communication channels.

-
- [1] H. P. Yuen, R. S. Kennedy, M. Lax, *Optimum testing of multiple hypotheses in quantum detection theory*, IEEE Trans. Inf. Theory, IT21, 125 (1975).
 - [2] C. W. Helstrom, *Quantum detection and estimation theory* (Academic Press, 1976).
 - [3] J. A. Bergou, U. Herzog and M. Hillery, *Discrimination of Quantum States*, Lect. Not. Phys. **649**, 415 (2004).
 - [4] A. Chefles, *Quantum States: Discrimination and Classical Information Transmission. A Review of Experimental Progress*, Lect. Not. Phys. **649**, 465 (2004).
 - [5] J. A. Bergou, *Discrimination of quantum states*, J. Mod. Opt. **57**, 160 (2010).
 - [6] I. D. Ivanovic, *How to differentiate between non-orthogonal states*, Phys. Lett. A **123**, 257 (1987);
 - [7] D. Dieks, *Overlap and distinguishability of quantum states*, Phys. Lett. A **126**, 303 (1988);
 - [8] A. Peres, *How to differentiate between non-orthogonal states*, Phys. Lett. A **128**, 19 (1988).
 - [9] N. Tomassoni, and M. G. A. Paris, *Quantum binary channels with mixed states*, Phys. Lett. A **373**, 61 (2008).
 - [10] G. Cariolaro, *Quantum communication* (Springer, 2015).
 - [11] K. Günthner, I. Khan, D. Elser, B. Stiller, Ö. Bayraktar, C. R. Müller, K. Saucke, D. Tröndle, F. Heine, S. Seel, P. Greulich, H. Zech, B. Gütlich, S. Philipp-May, C. Marquardt, and G. Leuchs, *Quantum-limited measurements of optical signals from a geostationary satellite*, Optica **4**, 611 (2017).
 - [12] E. Diamanti, H.-K. Lo, B. Qi, and Z. Yuan, *Practical challenges in quantum key distribution*, npj Quantum Information **2**, 16025 (2016).
 - [13] C. Wittmann, U. L. Andersen, M. Takeoka, D. Sych, and G. Leuchs, *Demonstration of Coherent-State Discrimination Using a Displacement-Controlled Photon-Number-Resolving Detector*, Phys. Rev. Lett. **104**, 100505 (2010).
 - [14] C. R. Müller, M. A. Usuga, C. Wittmann, M. Takeoka, C. Marquardt, U. L. Andersen, and G. Leuchs, *Quadrature phase shift keying coherent state discrimination via a hybrid receiver*, New J. of Phys. **14**, 083009 (2012).
 - [15] F. E. Becerra, J. Fan, G. Baumgartner, J. Goldhar, J. T. Kosloski, and A. Migdall, *Experimental demonstration of a receiver beating the standard quantum limit for multiple nonorthogonal state discrimination*, Nat. Phot. **7**, 147 (2013).
 - [16] F. E. Becerra, J. Fan, G. Baumgartner, S. V. Polyakov, J. Gold-

- har, J. T. Kosloski, and A. Migdall *M-ary-state phase-shift-keying discrimination below the homodyne limit*, Phys. Rev. A **84**, 062324 (2011).
- [17] R. Nair, B. J. Yen, S. Guha, J. H. Shapiro, and S. Pirandola, *Symmetric M-ary phase discrimination using quantum-optical probe states*, Phys. Rev. A **86**, 022306 (2012).
- [18] M. G. A. Paris, *Nearly ideal binary communication in squeezed channels*, Phys. Rev. A **64**, 014304 (2001).
- [19] S. Izumi, M. Takeoka, K. Ema, and M. Sasaki, *Quantum receivers with squeezing and photon-number-resolving detectors for M-ary coherent state discrimination*, Phys. Rev. A **87**, 042328 (2013).
- [20] C.-W. Lau, V. A. Vilmrotter, S. Dolinar, J. M. Geremia, and H. Mabuchi, *Binary quantum receiver concept demonstration*, Proc. SPIE **6105**, Free-Space Laser Communication Technologies XVIII, 61050J (2006).
- [21] R. S. Kennedy, *A near-optimum receiver for the binary coherent state quantum channel*, RLE Progress Report **108**, 219 (1973).
- [22] S. J. Dolinar, Jr., *An optimum receiver for the binary coherent state quantum channel*, RLE Progress Report **111**, 115 (1973).
- [23] M. Bina, A. Allevi, M. Bondani, and S. Olivares, *Phase-reference monitoring in coherent-state discrimination assisted by a photon-number resolving detector*, Sci. Rep. **6**, 26025 (2016).
- [24] S. Olivares, S. Cialdi, F. Castelli, and M. G. A. Paris, *Homodyne detection as a near-optimum receiver for phase-shift-keyed binary communication in the presence of phase diffusion*, Phys. Rev. A **87**, 050303(R) (2013).
- [25] V. C. Usenko, and R. Filip, *Squeezed-state quantum key distribution upon imperfect reconciliation*, New J. of Phys. **13**, 113007 (2011).
- [26] H. A. Bachor, and T. Ralph, *A guide to Experiments in Quantum Optics* (Wiley-VCH Verlag, 2004).
- [27] S. Izumi, M. Takeoka, M. Fujiwara, N. Dalla Pozza, A. As-salini, K. Ema, and M. Sasaki, *Displacement receiver for phase-shift-keyed coherent states*, Phys. Rev. A **86**, 042328 (2012).
- [28] S. Izumi, M. Takeoka, K. Wakui, M. Fujiwara, K. Ema, and M. Sasaki, *Optical phase estimation via coherent state and displaced photon counting*, Phys. Rev. A **94**, 033842 (2016).
- [29] M. Bina, A. Allevi, M. Bondani, and S. Olivares, *Homodyne-like detection for coherent state-discrimination in the presence of phase noise*, Opt. Express **25**, 10685 (2017).
- [30] M. G. Genoni, S. Olivares, and M. G. A. Paris, *Optical phase estimation in the presence of phase diffusion*, Phys. Rev. Lett. **106**, 153603 (2011).
- [31] L. G. Kazovsky, G. Kalogerakis, and W. T. Shaw, *Homodyne phase-shift-keying systems: Past challenges and future opportunities*, J. Lightwave Technol. **24**, 4876 (2006).
- [32] S. Olivares, and M. G. A. Paris, *Binary optical communication in single-mode and entangled quantum noisy channels*, J. Opt. B: Quantum and Semiclass. Opt. **6**, 69 (2004).
- [33] C. Gardiner, and P. Zoller, *Quantum Noise*, (Springer, Berlin, 2004).
- [34] S. Olivares, *Quantum optics in the phase space*, Eur. Phys. J. Special Topics **203**, 3 (2012).
- [35] S. Cialdi, C. Porto, D. Cipriani, S. Olivares, and M. G. A. Paris, *Full quantum state reconstruction of symmetric two-mode squeezed thermal states via spectral homodyne detection and a state-balancing detector*, Phys. Rev. A **93**, 043805 (2016).
- [36] V. D'Auria, S. Fornaro, A. Porzio, S. Solimeno, S. Olivares, and M. G. A. Paris, *Full characterization of Gaussian bipartite entangled states by a single homodyne detector*, Phys. Rev. Lett. **102**, 020502 (2009).